Shock Tunnel Studies on Shock–Shock Interaction

Abhishek Khatta and Gopalan Jagadeesh

Introduction and Motivation

The interaction of a Shockwave with another Shockwave is an unavoidable phenomenon in high speed flows. These interactions may lead to high pressure and thermal loads on the surface in the vicinity, deteriorates the aerodynamic performance of the system if present internally, and may also lead to the un-start of Scramjet engine due to presence of the subsonic flow downstream of the interaction point. Edney [1] identified and classified these interactions into six different types using a blunt body in a Hypersonic Wind Tunnel. This phenomenon has motivated many research groups to study them and try to figure out the critical conditions for the pressure and thermal loads. Wieting and Holden [2] experimentally studied the shockwave interference heating on a cylinder at Mach 6 and Mach 8. Sanderson, Hornung, and Sturtevant [3] studied the interacting shockwaves in dissociating gas.

Most important feature of these interactions is the increase in the pressure and heat flux on the nearby surface, where the waves after the interaction meet the surface. Though much effort has been put both experimentally and computationally into the understanding of these interactions, only few groups lead the study in short duration facilities, where high enthalpy flows can be generated.

For the present work, the Hypersonic Shock Tunnel–2 (HST-2), at Laboratory of Hypersonic and Shock wave Research (LHSR), Indian Institute of Science, is used to generate a flow of Mach 5.64, obtained by the straight-through mode operation of the tunnel. Here, a wedge is used to generate a planar shock wave, which is allowed to interact with a bow shock formed in front of a hemispherical body. The model assembly is designed in such a way that keeping the hemispherical body fixed, the wedge can be moved, thereby changing the distance between the wedge tip and nose of hemispherical body. Different location of the wedge relative to the hemispherical body leads to the change in location on bow shock where the planar shock interacts with it. Thus, by changing the relative location of the wedge with respect to the hemispherical body makes the interaction point to move along the trajectory of the bow shock from a low subsonic region of the bow shock to the near normal region of the bow shock near the nose region. This leads to the formation of different interaction patterns which were classified by B. Edney [1] as Type I, Type-II, Type-III, Type-IV, Type-V, and Type VI. Present investigation aims at mapping the heat transfer rates and pressure distribution on the surface of hemispherical body in the presence of a planar oblique shock wave.

For all the experiments reported here, air is used as the test gas at 1.06 MJ/kg of total enthalpy at the following test conditions using HST-2.

Models are fabricated to allow the housing of Platinum thin film heat transfer gauges, along the centerline of the hemispherical body. The photographs of the model and the heat transfer gauges are shown in Figs. 1 and 2, respectively. Along with the Platinum Thin Film gauges, Kulite pressure transducers were mounted at discrete locations to map the time history of surface pressure on the hemispherical body. A schematic of the model assembly showing the dimensions of the model is shown in Fig. 3.

Simultaneous flow visualization, using schlieren technique, was done to understand and characterize different interaction patterns and the corresponding relation to the measured heat transfer rates and pressure distribution along the surface of the hemispherical body.

A. Khatta (✉) • G. Jagadeesh
Department of Aerospace Engineering, Indian Institute of Science, Bangalore 560012, India
e-mail: aabhi.ak@gmail.com

G. Ben-Dor et al. (eds.), *30th International Symposium on Shock Waves 1*, DOI 10.1007/978-3-319-46213-4_111

Table 1 Typical freestream conditions in HST2

Flow Mach no.	Pressure (kPa)	Temperature (K)	Density (kg/m^3)	Unit Reynold's No. (/m)
5.64	1.86	143.59	0.0508	6.98×10^6

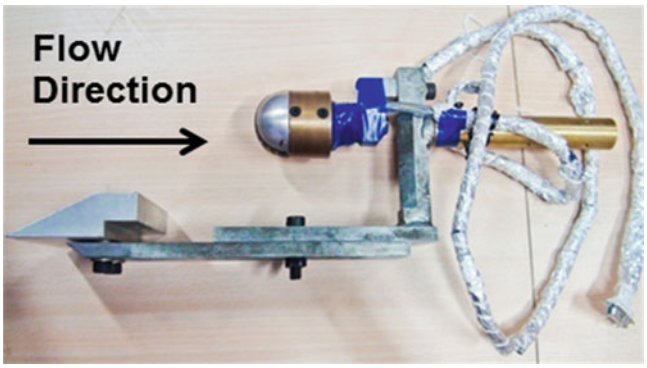

Fig. 1 Complete model assembly

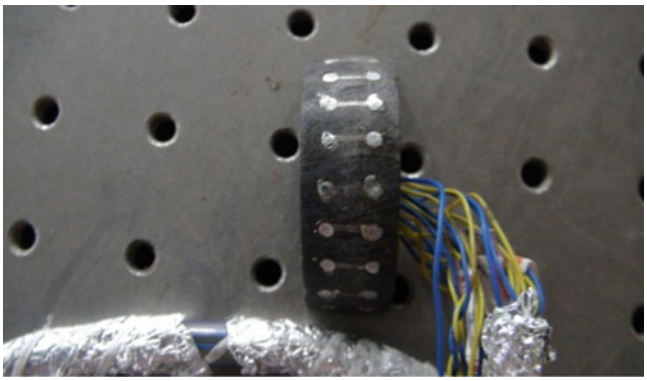

Fig. 2 Macor substrate with platinum thin film gauges on the surface

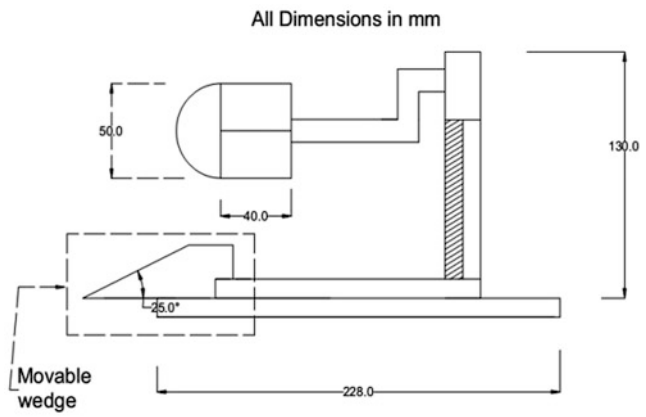

Fig. 3 Schematic drawing of model assembly

Results and Discussions

As the wedge is moved to provide different interaction point of the planar shock on the bow shock wave trajectory, the resulting interaction patterns are accompanied by different pressure distribution and heat transfer distribution on the surface. The different interaction patterns which were so obtained were identified through schlieren visualization and corresponding convective heat transfer distribution and pressure distribution on the surface were analyzed to throw light on the reasons for difference in measurements for different interactions.

One PCB Piezoelectronics pressure transducer was mounted at the nose point of the hemispherical body. Two Kulite pressure transducers were mounted, at 75° off from the nose with center of hemisphere as the reference. Sensor located close to the wedge is given the location −75°, while sensor located farther away from the wedge is given the location +75°.

TYPE-I Interaction

This type of interaction is obtained when the oblique shock interacts with the bow shock far away from the nose, such that the two shock waves are of different families and intensities of the impinging shock waves are almost same, the simplest type of interaction appears. Since the interaction happens outside the sonic region, the shock stand-off distance is unaltered when compared to the undisturbed case.

Pressure data obtained in TYPE-I interaction is taken as reference and all pressure values are normalized using the nose point surface pressure obtained in TYPE-I interaction. Figure 4a shows the normalized surface pressure distribution for TYPE-I interaction, where at vertical axis P_SI stands for measured pressure in presence of shock interaction and P__UD stands for measured pressure at nose point for TYPE-I interaction.

It can be seen from Fig. 1 that both pressure distribution and heat transfer distribution on the surface are having symmetrical distribution owing to the fact that bow shock around the hemispherical body is symmetrical as seen in the corresponding schlieren image.

TYPE-II Interaction

When the intensity of the bow shock wave increases as we go close to nose point, TYPE-II interaction appears, characterized by a normal shock, separating the oblique

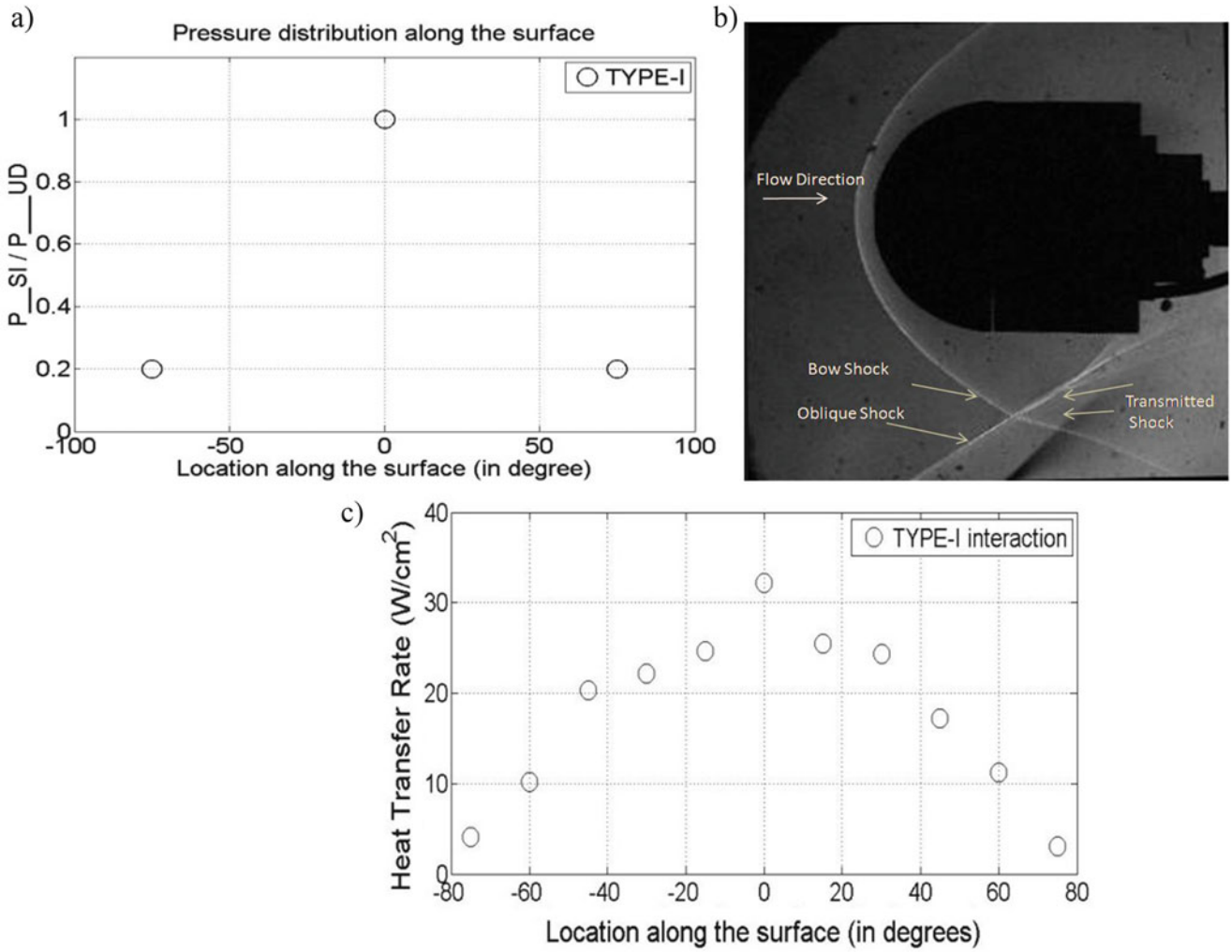

Fig. 4 (**a**) Pressure distribution along the surface of hemispherical body; (**b**) schlieren image showing TYPE-I interaction; (**c**) heat transfer distribution along the surface of hemispherical body

shock wave and bow shock wave. The shape of the shock elsewhere and the shock stand-off distance remains unchanged as the interaction is still far away from sonic line. Two triple points appear in the vicinity of the surface. The transmitted shock from one of the triple points is seen to hit the surface. Figure 5b shows the schlieren image of TYPE-II interaction. The normal shock is clearly seen and enlarged in the inset, where the transmitted shock is also seen to hit the surface of the hemispherical body. From the pressure distribution plot it can be seen that the presence of an additional wave near the bottom half of the hemispherical body tends to rise the surface pressure and destroys the symmetrical distribution. On the other hand, the surface heat transfer distribution is not much changed, and follows the trend of TYPE-I interaction.

TYPE-III Interaction

As the oblique shock impinges on the lower region of sonic circle, a slip line is formed separating the subsonic region behind the bow shock and supersonic region behind the transmitted shock. The slip line hits the body surface, and the presence of supersonic flow below the slip line causes the presence of shock wave off the surface. The shock pattern above the point of interaction is changed, and the bow shock is no more normal to the body surface at the nose point of the body. This is reflected in the surface pressure distribution plot as the normalized pressure at 0° is less when compared with that of TYPE-I interaction. The surface heat transfer distribution is greatly modified and lower half of the model experiences comparatively higher heat transfer rates. The

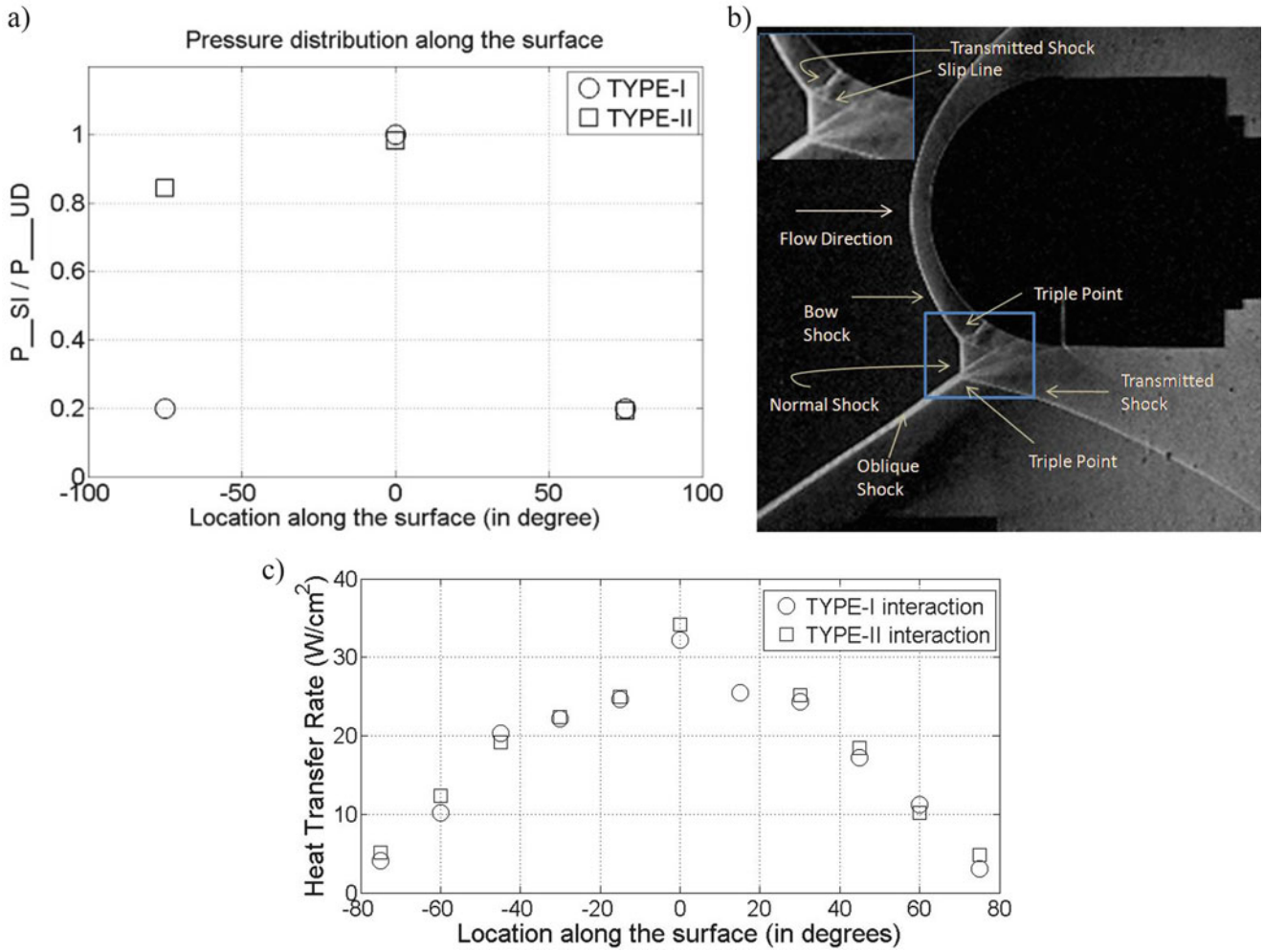

Fig. 5 (**a**) Pressure distribution along the surface of hemispherical body; (**b**) schlieren image showing TYPE-II interaction; (**c**) heat transfer distribution along the surface of hemispherical body

heat transfer rates on the upper half of the body follows the trends of TYPE-I interaction.

Conclusions

Shock–shock interaction studies were carried out in HST-2, at 5.64 Mach and total enthalpy of 1.06 Mj/kg. A hemispherical body of 50 mm diameter, made of aluminum, produced a bow shock when immersed in a hypersonic flow, and a wedge of 25° angle was used to generate planar oblique shock wave, which hits this bow shock. The wedge mounting assembly is made in such a way that the relative distance between the hemispherical body nose and the wedge tip can be changed from run to run. Depending upon the location on bow shock where the oblique shock hits, different interaction patterns are observed. Schlieren visualization was performed to analyze the flow structures generated during different interactions and simultaneously, pressure measurement and convective heat transfer measurement on the surface along the centerline of the hemispherical body was made to correlate with the schlieren images.

It was seen that TYPE-I interaction gives symmetrical distribution of both pressure distribution on the surface and heat transfer distribution on the surface. Since in TYPE-I interaction, the oblique shock wave and the bow shock wave meet far downstream and do not disturb the flow in the vicinity of the hemisphere, the measured values of surface pressure and measure heat transfer rates for all interactions were compared with those of TYPE-I interaction. The presence of additional waves in TYPE-II interaction causes the surface pressure distribution to deviate from symmetrical distribution, but the heat transfer distribution is not much disturbed and follows the trends of TYPE-I interaction. Type-III interaction leads to the change of shock shape above the point of interaction between the oblique shock wave and the bow shock wave, and this leads to the reduction of the surface pressure at the nose point of

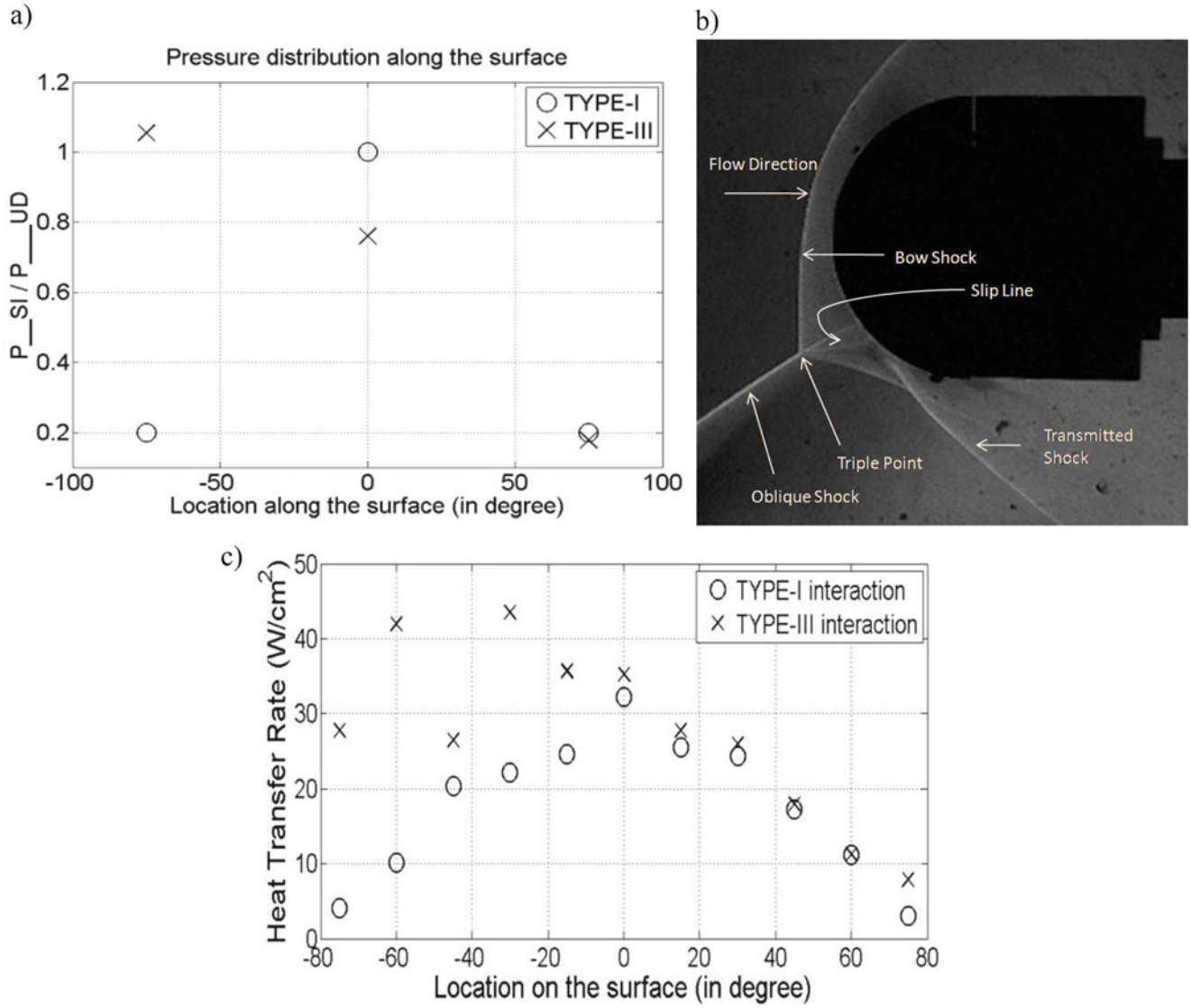

Fig. 6 (**a**) Pressure distribution along the surface of hemispherical body; (**b**) schlieren image showing TYPE-III interaction; (**c**) heat transfer distribution along the surface of hemispherical body

hemispherical body. The measured heat transfer rate on the surface also shows deviation and increase in the values as compared to TYPE-I interaction, at the bottom half of the hemispherical body.

The study and analyses of TYPE-IV, TYPE-V, and TYPE-VI interaction patterns will be presented during the conference.

References

1. Edney, B.: Effects of shock impingement on heat transfer around blunt bodies. AIAA J. **6**(1), 15–21 (1968)
2. Wieting, A.R., Holden, M.S.: Experimental shock-wave interference heating on a cylinder at Mach 6 and Mach 8. AIAA J. **27**, 1557–1565 (1989)
3. Sanderson, S.R., Hornung, H.G., Sturtevant, B.: Aspects of planar, oblique and interacting shock waves in an ideal dissociating gas. Phys. Fluids **15**, 1638–1649 (2003)